Negative Thermal Expansion Hot Paper

International Edition: DOI: 10.1002/anie.201702955
German Edition: DOI: 10.1002/ange.201702955

Switching Between Giant Positive and Negative Thermal Expansions of a $YFe(CN)_6$-based Prussian Blue Analogue Induced by Guest Species

Qilong Gao, Jun Chen, Qiang Sun, Dahu Chang, Qingzhen Huang, Hui Wu, Andrea Sanson, Ruggero Milazzo, He Zhu, Qiang Li, Zhanning Liu, Jinxia Deng, and Xianran Xing*

Abstract: *The control of thermal expansion of solid compounds is intriguing but remains challenging. The effect of guests on the thermal expansion of open-framework structures was investigated. Notably, the presence of guest ions (K^+) and molecules (H_2O) can substantially switch thermal expansion of $YFe(CN)_6$ from negative ($\alpha_v = -33.67\times10^{-6}\,K^{-1}$) to positive ($\alpha_v = +42.72\times10^{-6}\,K^{-1}$)—a range that covers the thermal expansion of most inorganic compounds. The mechanism of such substantial thermal expansion switching is revealed by joint studies with synchrotron X-ray diffraction, X-ray absorption fine structure, neutron powder diffraction, and density functional theory calculations. The presence of guest ions or molecules plays a critical damping effect on transverse vibrations, thus inhibiting negative thermal expansion. An effective method is demonstrated to control the thermal expansion in open-framework materials by adjusting the presence of guests.*

The issue of controlling thermal expansion is vital but remains challenging.[1–5] The occurrence of negative thermal expansion (NTE) materials offers a promising possibility. In 1968, Hummel et al. first observed the NTE phenomenon in the framework material ZrW_2O_8.[6] However, a possible mechanism for NTE was not revealed until 1996, when Sleight et al. solved the crystal structure of ZrW_2O_8 and elucidated the interesting NTE phenomenon,[1] which proposed rigid unit modes (RUMs) as the origin of NTE. Subsequently, many more NTE framework materials were found, such as oxides containing M–O–M oxygen atom bridges with the general chemical formulae AMO_5,[7] $A_2M_3O_{12}$,[8,9] AO_3,[10] AM_2O_7,[11] and AM_2O_8;[1,12] ReO_3-type fluorides,[13–16] cyanides, and the Prussian blue analogues formed by double atom M-C≡N-M bridges in $Zn(CN)_2$,[17] $Ag_3Co(CN)_6$,[18] $LnCo(CN)_6$,[19] and $FeCo(CN)_6$;[20] and metal–organic frameworks (MOFs)[21–24] with carboxylate linkages.

The control of thermal expansion in NTE materials was mainly achieved by chemical substitution, as reported in previous studies.[25–27] Since chemical substitution can have a pronounced effect on electronic and crystal structures, thermal expansion can be well-controlled—especially in electronically driven NTE materials, such as magnetic anti-perovskite manganese nitrides,[28,29] $PbTiO_3$-based ferroelectrics,[30–32] and intermetallic charge-transfer compounds of $BiNiO_3$ and $LaCu_3Fe_4O_{12}$.[33–35] However, in open-framework materials, chemical substitution might not be a direct method to adjust thermal expansion, because the NTE of such materials is associated with the lattice dynamics rather than the electronic structures. For example, the linear coefficient of thermal expansion (CTE, α_l) for $Zr_{1-x}M_xW_2O_{8-y}$ (M = Sc, In, Y) materials only varies over a narrow range (-7.3 to $-8.7\times10^{-6}\,K^{-1}$).[36] In contrast, it is well-known that NTE of open-framework structures originates from transverse thermal vibrations of atoms (for example, ZrW_2O_8[37,38] and ScF_3[39]). Such transverse thermal vibrations should be reduced or hindered if guest ions or molecules exist in the empty spaces of a framework. We notice that there are some interesting previous studies that demonstrate that the thermal expansion of framework materials changes extensively because of the presence of guest molecules. For example, NTE disappears in ZrW_2O_8 in the presence of H_2O molecules (for $ZrW_2O_8{\cdot}0.55\,H_2O$: $\alpha_l = 1.9\times10^{-6}\,K^{-1}$, 15–298 K).[40] Thermal expansion changes substantially after the insertion of H_2O into $ZnPt(CN)_6$.[41] It is groundbreaking that the insertion and the removal of CCl_4 guest molecules furnishes thermal expansion switching between negative and positive in $Cd(CN)_2$.[42] Similar interesting phenomena were also observed in MOFs.[24,43] Recently, we successfully controlled thermal expansion in simple ScF_3-based NTE materials from negative, to zero, to positive, by insertion and removal of Li ions.[44]

Herein, we demonstrate that the thermal expansion of $YFe(CN)_6$-based Prussian blue analogues can be switched substantially from negative to positive by introduction of guest molecules (H_2O) and ions (K^+) to the void spaces of its framework structure. Crystal structures and thermal expansions were determined by high-resolution synchrotron X-ray diffraction (SXRD), neutron powder diffraction (NPD), and from the temperature dependence of XRD. The role of the

[*] Q. L. Gao, Prof. J. Chen, H. Zhu, Q. Li, Z. N. Liu, Prof. J. X. Deng, Prof. X. R. Xing
Department of Physical Chemistry
University of Science and Technology Beijing
Beijing 100083 (China)
E-mail: junchen@ustb.edu.cn
Prof. Q. Sun, D. H. Chang
International Laboratory for Quantum Functional Materials of Henan, School of Physics and Engineering, Zhengzhou University
Zhengzhou, 450001 (China)
Dr. Q. Z. Huang, Dr. H. Wu
NIST Center for Neutron Research
National Institute of Standards and Technology
Gaithersburg, MD 20899-6102 (USA)
Prof. A. Sanson, Dr. R. Milazzo
Department of Physics and Astronomy, University of Padova
35131 Padova (Italy)

Supporting information for this article can be found under: https://doi.org/10.1002/anie.201702955.

guest ions and molecules upon switching of the thermal expansion is explained by the solid state structure and the characteristics of the lattice dynamics. The present approach permits tailoring of thermal expansion and may be extended to many other NTE framework materials.

The crystal structures of hydrated samples of $YFe(CN)_6{\cdot}4H_2O$ and $KYFe(CN)_6{\cdot}3H_2O$ were investigated by high-resolution SXRD (Supporting Information, Figures S1,2 and Tables S1,2) and those of the $YFe(CN)_6$ and $KYFe(CN)_6$ samples by in situ XRD after dehydration (Supporting Information, Figures S3,4 and Tables S3,4). Figure 1 shows the structures of hydrated and dehydrated $YFe(CN)_6{\cdot}4H_2O$ and $KYFe(CN)_6{\cdot}3H_2O$ and their transformations. YN_6 and FeC_6 polyhedra in the host framework structure are bridged by CN units (Figure 1 a). Insertion of the guest K^+ ions and H_2O molecules into the pores of the host framework has a different effect on the structure symmetry. K^+ ions have a relatively small effect (compare $YFe(CN)_6{\cdot}4H_2O$ (*Cmcm*) and $KYFe(CN)_6{\cdot}3H_2O$ (*Pbnm*)), while H_2O molecules have a large effect and convert the hexagonal $YFe(CN)_6$ structure ($P6_3/mmc$) to the orthorhombic $YFe(CN)_6{\cdot}4H_2O$ (*Cmcm*) structure.

The refined structure of $YFe(CN)_6$ is consistent with that previously reported.[45] The Y atom coordinates to six N atoms to form a bicapped distorted trigonal prism (YN_6), while the Fe atom retains the usual regular octahedral coordination geometry (FeC_6). The YN_6 and FeC_6 groups in the entire structure of $YFe(CN)_6$ are bridged through CN units (Figure 1 a). The M-CN-M linkage of $YFe(CN)_6$ is near linear (the angle of Y-N-Fe and Y-C-Fe linkages is 176.01(1)° and 179.60(1)°, respectively), which is the same as that reported for other Prussian blue analogues, such as $FeCo(CN)_6$[20] and $ZnPt(CN)_6$.[41] $YFe(CN)_6$ is very hygroscopic because it possesses large pore spaces. $YFe(CN)_6$ easily absorbs H_2O and transforms into the hydrated complex $YFe(CN)_6{\cdot}4H_2O$ (Figure 1 b). After hydration the coordination number of Y^{3+} changes from six to eight, and the resultant YN_6O_2 and FeC_6 polyhedra are linked by CN units (Figure 1 b).

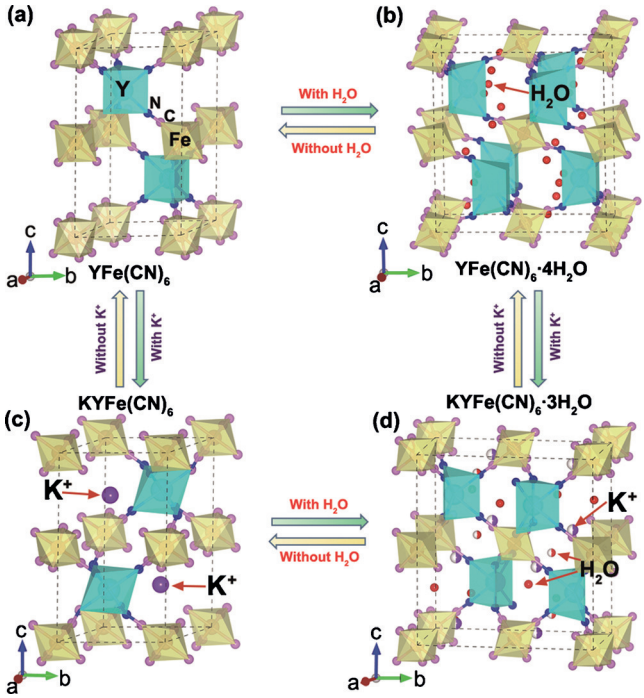

Figure 1. Crystal structure of $YFe(CN)_6$-based Prussian blue analogues with or without guest K^+ ions and H_2O molecules: a) $YFe(CN)_6$ ($P6_3/mmc$), b) $YFe(CN)_6{\cdot}4H_2O$ (*Cmcm*), c) $KYFe(CN)_6$ ($P\bar{3}1c$), and d) $KYFe(CN)_6{\cdot}3H_2O$ (*Pbnm*). Polyhedra key: FeC_6 (yellow), YN_6 (light blue).

The crystal structure of $KYFe(CN)_6{\cdot}3H_2O$ is shown in Figure 1 d, in which one K^+ ion substitutes one H_2O molecule in $YFe(CN)_6{\cdot}4H_2O$. K^+ ions and water molecules are located above and below the YN_6 trigonal prism near the $z = 0$ and 1/2 planes in the structure. $KYFe(CN)_6{\cdot}3H_2O$ exhibits a three-dimensional network consisting of corner-sharing FeC_6 and YN_6O_3 polyhedra. After dehydration, the structure shows a dramatic transformation from the orthorhombic (No.62, *Pbnm*) $KYFe(CN)_6{\cdot}3H_2O$ to the hexagonal (No.163, $P\bar{3}1c$) $KYFe(CN)_6$.[46] The YN_6O_3 structure restores to perfect YN_6 octahedral coordination geometry and K^+ ions migrate to one crystallographic site (Figure 1 c). Meanwhile, the unit cell volume of $KYFe(CN)_6$ (516.316 Å^3) dramatically contracts by 18.3 % compared to that of $YFe(CN)_6$ (632.337 Å^3), and the Fe-CN-Y bond angles contract (the Y-N-Fe angle is 140.54(5)°).

Notably, the structural transformation of hydrated and dehydrated samples is fully reversible (Supporting Information, Figure S7). There are two types of water in both $YFe(CN)_6{\cdot}4H_2O$ and $KYFe(CN)_6{\cdot}3H_2O$; namely, uncoordinated and coordinated water, which are presented in the crystal structure (Figure 1 b,d), thermogravimetric analysis–differential scanning calorimetry (TGA-DSC; Supporting Information, Figure S8), and FTIR vibrational modes (Supporting Information, Figure S9). For both $YFe(CN)_6{\cdot}4H_2O$ and $KYFe(CN)_6{\cdot}3H_2O$, there are two sharp exothermic peaks during the thermal decomposition (Supporting Information, Figure S8). The high frequency ν(OH) band in the region near 3610–3540 cm^{-1} is ascribed to coordinated water molecules, while the broad stretching bands near the region 3450–3260 cm^{-1} belong to uncoordinated water.[47,48]

To maintain charge balance, the valence of Fe changes upon insertion of K^+ ions. Herein, we have studied this effect on the air-stable hydrated samples of $YFe(CN)_6{\cdot}4H_2O$ and $KYFe(CN)_6{\cdot}3H_2O$. Figure 2 shows the room-temperature spectra of Y 3d X-ray photoelectron spectroscopy (XPS) and Fe K-edge X-ray absorption near-edge structure (XANES). No change in the Y 3d XPS spectra means that the chemical valence of Y remains stable. By contrast, the Fe K-edge X-ray absorption edge of $KYFe(CN)_6{\cdot}3H_2O$ is shifted by 1 eV to lower energy with respect to $YFe(CN)_6{\cdot}4H_2O$. This indicates that Fe^{3+} is reduced to Fe^{2+} after the insertion of K^+ ions, since the same Fe K-edge energy shift was observed in $K_3Fe(CN)_6$ and $K_4Fe(CN)_6$.[49] The K^+ ions can be inserted into the pores of $YFe(CN)_6$ easily because of such Fe valence reduction. Additionally, a remarkable difference has been observed in the band gap of $KYFe(CN)_6{\cdot}3H_2O$ ($E_g = 3.12$ eV) and $YFe(CN)_6{\cdot}4H_2O$ ($E_g = 1.86$ eV; Supporting Information, Figure S10).

It is intriguing that thermal expansion of $YFe(CN)_6$ can be switched substantially between negative and positive by guest

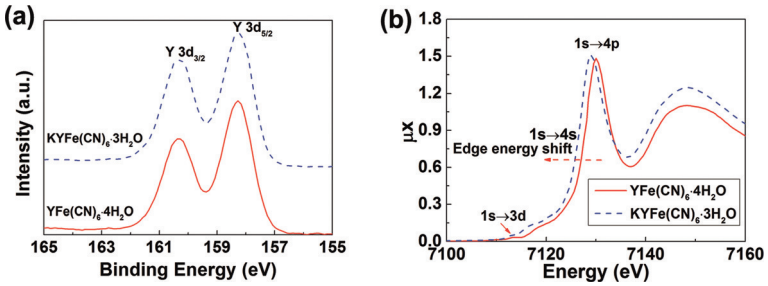

Figure 2. a) Y 3d XPS, and b) Fe K-edge XANES spectra for YFe(CN)6·4 H_2O and KYFe(CN)6·3 H_2O at room temperature.

K^+ ions and H_2O molecules (Figure 3; Supporting Information, Table S5). For $YFe(CN)_6$ without any guest ions or molecules, a strong NTE was observed along all crystal axes ($\alpha_v = -33.7\times10^{-6}\,K^{-1}$, $\alpha_a = -11.92\times10^{-6}\,K^{-1}$, $\alpha_c = -9.94\times10^{-6}\,K^{-1}$). This NTE, here observed for the first time, is larger than the isotropic NTE of the most popular ZrW_2O_8[1] and ScF_3 materials,[14] and comparable with that of other framework structures such as $CdPt(CN)_6$,[50] $LaCo(CN)_6$,[19] and $Cd(CN)_2$[51] (Supporting Information, Table S6). However, as soon as guest H_2O molecules are introduced into the framework of $YFe(CN)_6$, the thermal expansion is immediately switched to positive for $YFe(CN)_6{\cdot}4H_2O$ ($\alpha_v = +13.09\times10^{-6}\,K^{-1}$); the *b* and *c* axes show positive thermal expansion (PTE; $\alpha_b = +22.08\times10^{-6}\,K^{-1}$, and $\alpha_c = +13.09\times10^{-6}\,K^{-1}$) while the *a* axis retains NTE ($\alpha_a = -7.49\times10^{-6}\,K^{-1}$). With further introduction of K^+ ions, an even stronger PTE is achieved in $KYFe(CN)_6{\cdot}3H_2O$ ($\alpha_v = +42.72\times10^{-6}\,K^{-1}$); all axes display PTE ($\alpha_a = +25.67\times10^{-6}\,K^{-1}$, $\alpha_b = +12.27\times10^{-6}\,K^{-1}$, and $\alpha_c = +4.71\times10^{-6}\,K^{-1}$). Interestingly, the switched PTE is even stronger than that of common oxides, such as $SrTiO_3$ ($\alpha_v = +34\times10^{-6}\,K^{-1}$)[52] and α-Al_2O_3 ($\alpha_v = +23.4\times10^{-6}\,K^{-1}$).[53] However, upon removal of H_2O molecules from $KYFe(CN)_6{\cdot}3H_2O$ to obtain $KYFe(CN)_6$, the PTE is reduced by almost a half ($\alpha_v = +20.30\times10^{-6}\,K^{-1}$), with a NTE for the *c* axis ($\alpha_c = -3.43\times10^{-6}\,K^{-1}$) and a PTE for the other two axes ($\alpha_a = +11.84\times10^{-6}\,K^{-1}$). In the absence of K^+ ions, NTE appears again in $YFe(CN)_6$. As a result, we can switch the thermal expansion of the Prussian blue analogues over a giant CTE range by adjusting the concentration of guest ions or molecules.

Further experiments were performed on the thermal expansion of samples with hydration and dehydration cycling tests, and on $K_xYFe(CN)_6$ samples after partial removal of K^+ ions by electrochemical methods employed for K-ion batteries.[54] Thermal expansion can be reversibly switched from PTE of hydrated $YFe(CN)_6{\cdot}4H_2O$ to NTE of dehydrated $YFe(CN)_6$ (Supporting Information, Figure S11). Additionally, after partial extraction of K^+ ions, the $K_xYFe(CN)_6$ and $KYFe(CN)_6$ samples show the same structure, but thermal expansion is much reduced for the former ($\alpha_v = +3.2\times10^{-6}\,K^{-1}$; Supporting Information, Figure S12). We expect that future experiments concerning extraction and insertion of guest alkali metals will be directed by progress in the alkali-metal battery field.

Subsequently, we considered a mechanism to describe the role of guest ions and molecules on thermal expansion switching. Herein, we interpret such phenomena according to both structure and lattice dynamics by joint studies using NPD, extended X-ray absorption fine structure (EXAFS), and first-principle calculations. We suppose that the guest ions or molecules behave as a barrier to block the RUM-type vibrations or, in general, transverse vibrations (Supporting Information, Figure S13). Hence, we firstly adopt "atom–volume–density" (namely the volume of a single-atom occupancy) to quantify the relationship between guest and

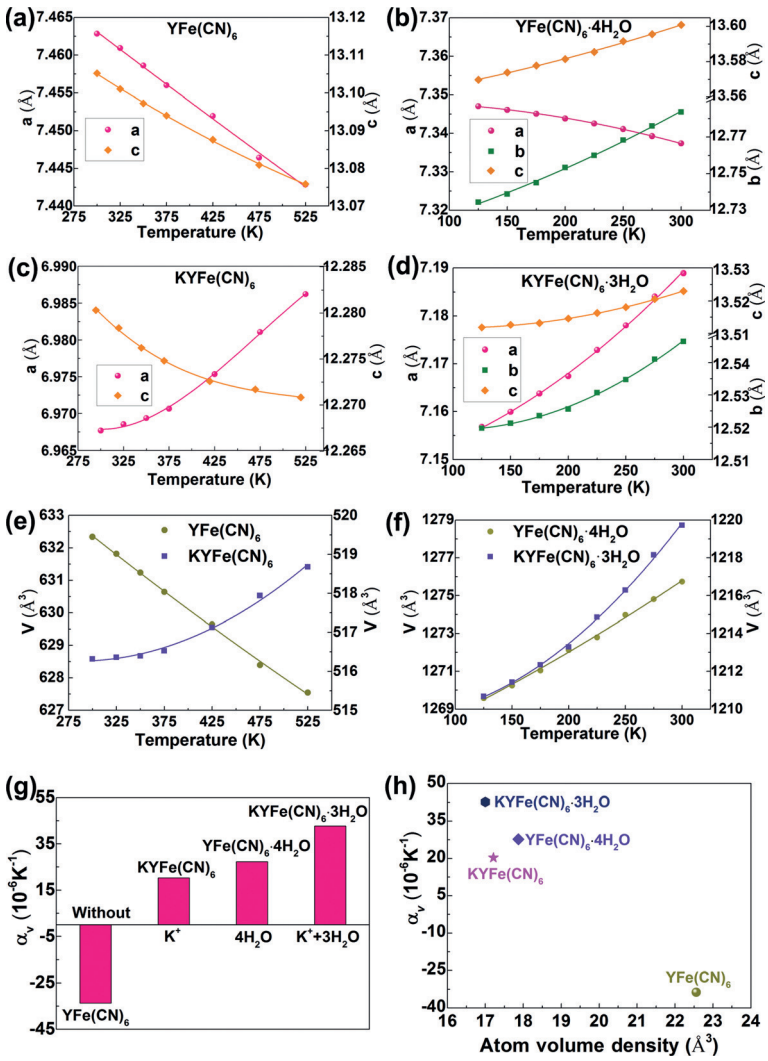

Figure 3. Temperature dependence of cell parameters and volumes for a) $YFe(CN)_6$, b) $YFe(CN)_6{\cdot}4H_2O$, c) $KYFe(CN)_6$, d) $KYFe(CN)_6{\cdot}3H_2O$, e) $YFe(CN)_6$ and $KYFe(CN)_6$, and f) $YFe(CN)_6{\cdot}4H_2O$ and $KYFe(CN)_6{\cdot}3H_2O$. g) CTE, α_v, in $YFe(CN)_6$ and related compounds. h) Correlation between atom–volume–density and α_v.

CTE. In this case, one water molecule or K^+ ion in the pore is considered as "one single atom" (a detailed analysis is tabulated in the Supporting Information, Table S7). As shown in Figure 3h, there is a correlation between atom–volume–density and CTE. That is, if there is enough space in the open-framework structure, the NTE arises because of the possibly strong transverse vibrations of bridging atoms. Otherwise, the transverse vibrations are reduced and thus NTE should be restrained or switched to PTE.

Firstly, the mechanism of such thermal expansion switching was studied experimentally by evaluating the anisotropic atomic displacement parameters (ADPs) of N and C atoms in PTE $YFe(CN)_6{\cdot}4H_2O$ and NTE $YFe(CN)_6$. We conducted NPD measurements, since N and C atoms are light elements. Refinement of the NPD data for $YFe(CN)_6{\cdot}4H_2O$ and $YFe(CN)_6$ is shown in Figures S5 and S6 (Supporting Information). As shown in Figure 4 and Figure S14 (Supporting Information), there are strong anisotropic ADPs in $YFe(CN)_6$, in which the transverse ADPs of N and C atoms are much larger than those of longitudinal ADPs. However, after the insertion of guest H_2O molecules, the ADPs are nearly identical for both transverse and longitudinal vibrations, which means that the transverse Fe–C and Y–N thermal vibrations are much hindered. Secondly, the atomic mean-square relative displacements (MSRDs)[55] determined by Fe K-edge EXAFS measurements, which also take into account the correlation of the atomic motion, indicate that there are much larger transverse Fe–C vibrations in NTE $YFe(CN)_6$ than in PTE $KYFe(CN)_6$ (Figure 4e,f; Supporting Information). In other words, K^+ ions have a damping effect on the transverse vibrations of C atoms, similar to H_2O molecules.

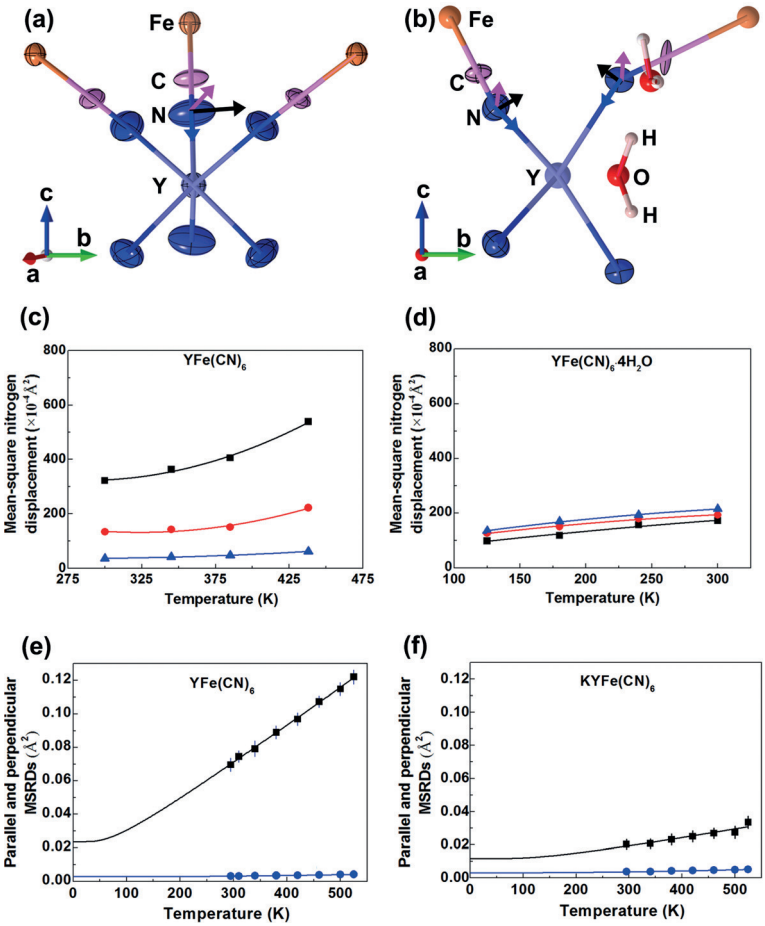

Figure 4. The ADPs depiction of N atoms in a) NTE $YFe(CN)_6$ and b) PTE $YFe(CN)_6{\cdot}4H_2O$ from NPD at 300 K. The ellipsoid size represents the amplitude of transverse and longitudinal vibrations of N and C atoms. Temperature variation of ADPs of the N atoms of c) $YFe(CN)_6$ and d) $YFe(CN)_6{\cdot}4H_2O$; transverse (⊥ Y-N-C-Fe axis (■), ⊥ Y-N-C-Fe axis (●)) and longitudinal (‖ Y-N-C-Fe axis (▲)). Perpendicular (⊥ Fe–C (■)) and parallel (‖ Fe–C (●)) MSRDs of the Fe–C atomic pairs measured by EXAFS in e) NTE $YFe(CN)_6$ and f) PTE $KYFe(CN)_6$. The solid lines are the corresponding best fit with the Einstein model.

To gain further insight into the mechanism by which guests tune the thermal expansion of $YFe(CN)_6$, density functional theory (DFT) calculations were carried out to study the lattice dynamics of two NTE $YFe(CN)_6$ and PTE $KYFe(CN)_6$ compounds. The space group of $YFe(CN)_6$ and $KYFe(CN)_6$ obtained from the experimental results was adopted in the calculations. The phonon dispersion and the mode Grüneisen parameters of the two compounds were calculated (see the Supporting Information for details). Figure 5a and 5b show the lowest transverse vibrational modes of NTE $YFe(CN)_6$ at 44 and 54.6 cm^{-1}, which exhibit the largest negative Grüneisen parameters and the main contribution to NTE (Figure 5c). The phonon density of states (DOS) of $YFe(CN)_6$ in the low-frequency range is strongly related to the vibrations of N atoms and, albeit in a minor way, to the vibrations of C atoms. (Supporting Information, Figure S18a). This suggests that the transverse vibrations of N and C atoms largely contribute to the NTE behavior of $YFe(CN)_6$, which is also indicated by the ADPs magnitude of N and C atoms. The NTE in the present $YFe(CN)_6$ supports the previous results that NTE arises from vibrational modes with negative mode Grüneisen parameters. In particular, the lowest energy optic modes contribute most to NTE of open-framework materials such as $Zn(CN)_2$,[56] ZrW_2O_8,[57] and ScF_3.[58] However, for PTE $KYFe(CN)_6$, the low-frequency contribution of N and, in part, of C atoms, is much weakened by the presence of K^+ ions (Supporting Information, Figure S18b). As a result, K^+ atoms have a strong effect on the vibrations of N and C atoms. Indeed the lowest energy mode of PTE $KYFe(CN)_6$ at 49.6 cm^{-1} has a small negative value, while the second lowest energy is positive (Figure 5d–g). From the comparison of Figures 4c and 4g, one can see that most vibrational modes with negative Grüneisen parameters in $YFe(CN)_6$ switch to positive when K^+ ions are inserted, thus resulting in PTE of $KYFe(CN)_6$.

In summary, the effect of guest ions and molecules on thermal expansion properties of the NTE open-framework $YFe(CN)_6$-based Prussian blue analogues was studied. We have discovered that the thermal expansion of $YFe(CN)_6$ can

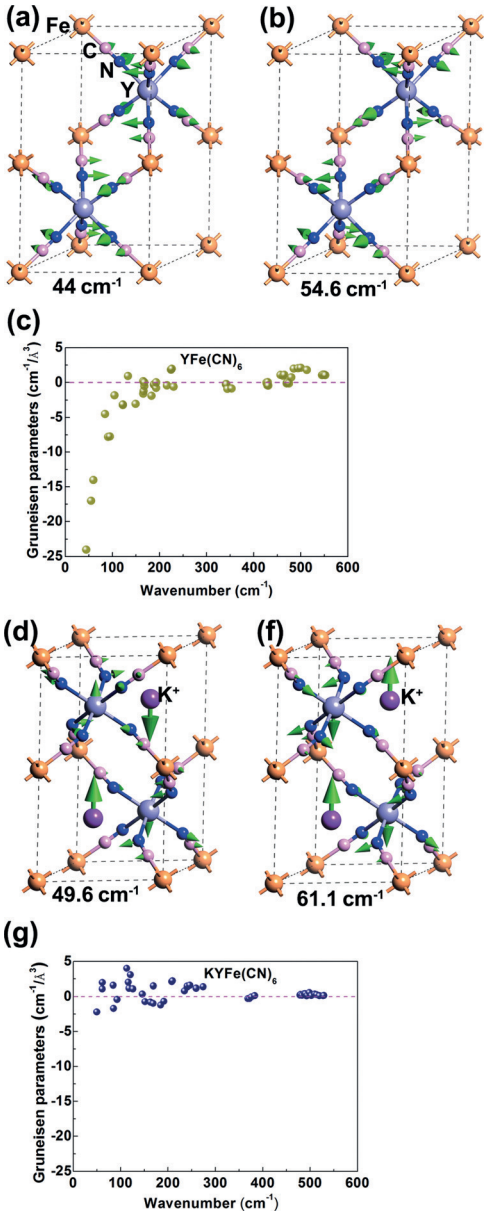

Figure 5. Depictions of the vibrational modes of Prussian blue analogues at low frequencies: NTE $YFe(CN)_6$ at a) 44 cm^{-1} and b) 54.6 cm^{-1}, and PTE $KYFe(CN)_6$ at d) 49.6 cm^{-1} and e) 61.1 cm^{-1}. Arrows indicate the vibrational directions of the atoms and the vibration amplitude is shown by the size of the arrow. The mode Grüneisen parameters of c) NTE $YFe(CN)_6$ and g) PTE $KYFe(CN)_6$ as a function of frequency.

be switched substantially from negative to positive by the addition of guest H_2O molecules or K^+ ions. The presence of water molecules and K^+ ions plays an important role in damping the transverse vibrations of C and N atoms, thus switching the thermal expansion from negative to positive. Concurrently, DFT calculations indicate that the negative Grüneisen parameters present in $YFe(CN)_6$ are suppressed by the presence of K^+ ions. This study demonstrates a technique for adjusting the CTE of NTE framework materials that may be applicable to other multifunctional materials.

Acknowledgements

This work was supported by the National Natural Science Foundation of China (grant nos. 91422301, 21231001, and 21590793), the Program for Changjiang Scholars and the Innovative Research Team in University (IRT1207), the Changjiang Young Scholars Award, National Program for Support of Top-notch Young Professionals, and the Fundamental Research Funds for the Central Universities, China (FRF-TP-14-012C1). The SXRD experiments were performed at the BL44B2 of SPring-8 with the approval of the Japan Synchrotron Radiation Research Institute (JASRI; proposal no. 2016A1060). EXAFS data were collected on the 1W1B beamline at Beijing Synchrotron Radiation Facility (BSRF) and at the BM08-LISA beamline of ESRF, Grenoble (experiment HC-3036). We acknowledge the technical assistance of the beamline scientists Dr. Kenichi Kato (JASRI), Dr. Lirong Zheng (BSRF), Dr. Francesco d'Acapito (LISA), and Dr. Alessandro Puri (LISA).

Conflict of interest

The authors declare no conflict of interest.

Keywords: crystal structures · density functional theory · negative thermal expansion · Prussian blue analogues · rigid unit modes

How to cite: *Angew. Chem. Int. Ed.* **2017**, *56*, 9023–9028
Angew. Chem. **2017**, *129*, 9151–9156

[1] T. A. Mary, J. S. O. Evans, T. Vogt, A. W. Sleight, *Science* **1996**, *272*, 90.
[2] P. Mohn, *Nature* **1999**, *400*, 18.
[3] K. Takenaka, *Sci. Technol. Adv. Mater.* **2012**, *13*, 013001.
[4] J. P. Attfield, *Nature* **2011**, *480*, 465.
[5] J. Chen, L. Hu, J. X. Deng, X. R. Xing, *Chem. Soc. Rev.* **2015**, *44*, 3522.
[6] C. Martinek, F. A. Hummel, *J. Am. Ceram. Soc.* **1968**, *51*, 227.
[7] X. W. Wang, Q. Z. Huang, J. X. Deng, R. B. Yu, J. Chen, X. R. Xing, *Inorg. Chem.* **2011**, *50*, 2685.
[8] J. S. O. Evans, T. A. Mary, A. W. Sleight, *J. Solid State Chem.* **1997**, *133*, 580.
[9] T. A. Mary, A. W. Sleight, *J. Mater. Res.* **1999**, *14*, 912.
[10] T. Chatterji, P. F. Henry, R. Mittal, S. L. Chaplot, *Phys. Rev. B* **2008**, *78*, 134105.
[11] V. Korthuis, N. Khosrovani, A. W. Sleight, N. Roberts, R. Dupree, W. J. Warren, *Chem. Mater.* **1995**, *7*, 412.
[12] S. E. Tallentire, F. Child, I. Fall, L. Vella-Zarb, I. R. Evans, M. G. Tucker, D. A. Keen, C. Wilson, J. S. Evans, *J. Am. Chem. Soc.* **2013**, *135*, 12849.
[13] B. K. Greve, K. L. Martin, P. L. Lee, P. J. Chupas, K. W. Chapman, A. P. Wilkinson, *J. Am. Chem. Soc.* **2010**, *132*, 15496.
[14] L. Hu, J. Chen, L. L. Fan, Y. Ren, Y. C. Rong, Z. Pan, J. X. Deng, R. B. Yu, X. R. Xing, *J. Am. Chem. Soc.* **2014**, *136*, 13566.
[15] J. C. Hancock, K. W. Chapman, G. J. Halder, C. R. Morelock, B. S. Kaplan, L. C. Gallington, A. Bongiorno, C. Han, S. Zhou, A. P. Wilkinson, *Chem. Mater.* **2015**, *27*, 3912.
[16] L. Hu, J. Chen, J. L. Xu, N. Wang, F. Han, Y. Ren, L. F. Li, X. R. Xing, *J. Am. Chem. Soc.* **2016**, *138*, 14530.
[17] K. W. Chapman, P. J. Chupas, C. J. Kepert, *J. Am. Chem. Soc.* **2005**, *127*, 15630.

[18] A. L. Goodwin, M. Calleja, M. J. Conterio, M. T. Dove, J. S. Evans, D. A. Keen, L. Peters, M. G. Tucker, *Science* **2008**, *319*, 794.
[19] S. G. Duyker, V. K. Peterson, G. J. Kearley, A. J. Ramirez-Cuesta, C. J. Kepert, *Angew. Chem. Int. Ed.* **2013**, *52*, 5266; *Angew. Chem.* **2013**, *125*, 5374.
[20] S. Margadonna, K. Prassides, A. N. Fitch, *J. Am. Chem. Soc.* **2004**, *126*, 15390.
[21] D. Dubbeldam, K. S. Walton, D. E. Ellis, R. Q. Snurr, *Angew. Chem.* **2007**, *119*, 4580.
[22] S. S. Han, W. A. Goddard, *J. Phys. Chem. C* **2007**, *111*, 15185.
[23] P. Lama, R. K. Das, V. J. Smith, L. J. Barbour, *Chem. Commun.* **2014**, *50*, 6464.
[24] I. Grobler, V. J. Smith, P. M. Bhatt, S. A. Herbert, L. J. Barbour, *J. Am. Chem. Soc.* **2013**, *135*, 6411.
[25] K. Takenaka, H. Takagi, *Appl. Phys. Lett.* **2005**, *87*, 261902.
[26] C. R. Morelock, B. K. Greve, L. C. Gallington, K. W. Chapman, A. P. Wilkinson, *J. Appl. Phys.* **2013**, *114*, 213501.
[27] M. S. Senn, C. A. Murray, X. Luo, L. Wang, F. T. Huang, S. W. Cheong, A. Bombardi, C. Ablitt, A. A. Mostofi, N. C. Bristowe, *J. Am. Chem. Soc.* **2016**, *138*, 5479.
[28] K. Takenaka, K. Asano, M. Misawa, H. Takagi, *Appl. Phys. Lett.* **2008**, *92*, 011927.
[29] C. Wang, L. H. Chu, Q. R. Yao, Y. Sun, M. M. Wu, L. Ding, J. Yan, Y. Y. Na, W. H. Tang, G. N. Li, Q. Z. Huang, J. W. Lynn, *Phys. Rev. B* **2012**, *85*, 220103.
[30] J. Chen, X. R. Xing, C. Sun, P. H. Hu, R. B. Yu, X. W. Wang, L. H. Li, *J. Am. Chem. Soc.* **2008**, *130*, 1144.
[31] J. Chen, L. L. Fan, Y. Ren, Z. Pan, J. Deng, R. Yu, X. R. Xing, *Phys. Rev. Lett.* **2013**, *110*, 115901.
[32] J. Chen, F. F. Wang, Q. Z. Huang, L. Hu, X. P. Song, J. X. Deng, R. B. Yu, X. R. Xing, *Sci. Rep.* **2013**, *3*, 2458.
[33] I. Yamada, K. Tsuchida, K. Ohgushi, N. Hayashi, J. Kim, N. Tsuji, R. Takahashi, M. Matsushita, N. Nishiyama, T. Inoue, T. Irifune, K. Kato, M. Takata, M. Takano, *Angew. Chem. Int. Ed.* **2011**, *50*, 6579; *Angew. Chem.* **2011**, *123*, 6709.
[34] M. Azuma, W. T. Chen, H. Seki, M. Czapski, K. Oka, M. Mizumaki, T. Watanuki, N. Ishimatsu, N. Kawamura, S. Ishiwata, M. G. Tucker, Y. Shimakawa, J. P. Attfield, *Nat. Commun.* **2011**, *2*, 347.
[35] Y. W. Long, V. Hayashi, T. Saito, M. Azuma, S. Muranaka, Y. Shimakawa, *Nature* **2009**, *458*, 60.
[36] N. Nakajima, Y. Yamamura, T. Tsuji, *Solid State Commun.* **2003**, *128*, 193.
[37] A. Sanson, *Chem. Mater.* **2014**, *26*, 3716.
[38] M. G. Tucker, A. L. Goodwin, M. T. Dove, D. A. Keen, S. A. Wells, J. S. Evans, *Phys. Rev. Lett.* **2005**, *95*, 255501.
[39] L. Hu, J. Chen, A. Sanson, H. Wu, C. Guglieri Rodriguez, L. Olivi, Y. Ren, L. L. Fan, J. X. Deng, X. R. Xing, *J. Am. Chem. Soc.* **2016**, *138*, 8320.
[40] N. Duan, U. Kameswari, A. W. Sleight, *J. Am. Chem. Soc.* **1999**, *121*, 10432.
[41] A. L. Goodwin, K. W. Chapman, C. J. Kepert, *J. Am. Chem. Soc.* **2005**, *127*, 17980.
[42] A. E. Phillips, A. L. Goodwin, G. J. Halder, P. D. Southon, C. J. Kepert, *Angew. Chem. Int. Ed.* **2008**, *47*, 1396; *Angew. Chem.* **2008**, *120*, 1418.
[43] H. L. Zhou, Y. B. Zhang, J. P. Zhang, X. M. Chen, *Nat. Commun.* **2015**, *6*, 6917.
[44] J. Chen, Q. L. Gao, A. Sanson, X. X. Jiang, Q. Z. Huang, A. Carnera, C. G. Rodriguez, L. Olivi, L. Wang, L. Hu, K. Lin, Y. Ren, Z. S. Lin, C. Wang, L. Gu, J. X. Deng, J. P. Attfield, X. R. Xing, *Nat. Commun.* **2017**, *8*, 14441.
[45] S. G. Duyker, V. K. Peterson, G. J. Kearley, A. J. Studer, C. J. Kepert, *Nat. Chem.* **2016**, *8*, 270.
[46] S. G. Duyker, G. J. Halder, P. D. Southon, D. J. Price, A. J. Edwards, V. K. Peterson, C. J. Kepert, *Chem. Sci.* **2014**, *5*, 3409.
[47] D. M. Gil, M. C. Navarro, M. C. Lagarrigue, J. Guimpel, R. E. Carbonio, M. I. Gómez, *J. Mol. Struct.* **2011**, *1003*, 129.
[48] J. M. Farmer, D. F. Mullica, J. A. Kautz, *J. Coord. Chem.* **2000**, *49*, 325.
[49] A. Bleuzen, C. Lomenech, V. Escax, F. Villain, F. Varret, C. Cartier dit Moulin, M. Verdaguer, *J. Am. Chem. Soc.* **2000**, *122*, 6648.
[50] K. W. Chapman, P. J. Chupas, C. J. Kepert, *J. Am. Chem. Soc.* **2006**, *128*, 7009.
[51] A. L. Goodwin, C. J. Kepert, *Phys. Rev. B* **2005**, *71*, 140301.
[52] X. R. Xing, J. Chen, J. X. Deng, G. R. Liu, *J. Alloys Compd.* **2003**, *360*, 286.
[53] M. Munro, *J. Am. Ceram. Soc.* **1997**, *80*, 1919.
[54] L. Xue, Y. Li, H. Gao, W. Zhou, X. Lü, W. Kaveevivitchai, A. Manthiram, J. B. Goodenough, *J. Am. Chem. Soc.* **2017**, *139*, 2164.
[55] P. Fornasini, R. Grisenti, *J. Synchrotron Radiat.* **2015**, *22*, 1242.
[56] K. W. Chapman, M. Hagen, C. J. Kepert, P. Manuel, *Phys. B: Condensed Matter* **2006**, *385*, 60.
[57] R. Mittal, M. Zbiri, H. Schober, E. Marelli, S. J. Hibble, A. M. Chippindale, S. L. Chaplot, *Phys. Rev. B* **2011**, *83*, 024301.
[58] C. W. Li, X. Tang, J. A. Munoz, J. B. Keith, S. J. Tracy, D. L. Abernathy, B. Fultz, *Phys. Rev. Lett.* **2011**, *107*, 195504.

Manuscript received: March 21, 2017
Revised manuscript received: May 31, 2017
Accepted manuscript online: June 8, 2017
Version of record online: June 23, 2017

